International Journal of GEOMATE, May, 2020, Vol.18, Issue 69, pp. 59 - 66
ISSN: 2186-2982 (P), 2186-2990 (O), Japan, DOI: https://doi.org/10.21660/2020.69.9125
Geotechnique, Construction Materials and Environment

CHARACTERIZING PORE-STRUCTURAL PARAMETERS OF VOLCANIC ASH SOIL: COMPARISON BETWEEN NON-DESTRUCTIVE AND INDIRECT METHODS

*Arjun BANIYA[1], Akihiro MATSUNO[1], and Ken KAWAMOTO[1]

[1]Graduate School of Science and Engineering, Saitama University, Japan.

*Corresponding Author, Received: 07 June 2019, Revised: 27 Nov. 2019, Accepted: 06 Feb. 2020

ABSTRACT: Mass transport within porous media is governed by their pore networks, which is highly influenced by pore structure parameters such as pore size distribution, porosity, pore tortuosity and pore coordination number. Micro-focus X-ray computed tomography (MFXCT) has emerged as a powerful non-destructive tool for the direct visualization and better understand soil pore geometry. In this study, soil macropore networks (typically, pore diameter ≥ 30 μm) were visualized and gas transport parameters were measured for volcanic ash soils taken from Nishi Tokyo City, Japan. Especially, the study aimed to identify the effect of moisture content on pore structural parameters based on MFXCT analysis and compare the MFXCT derived parameters to indirectly-estimated parameters from soil gas diffusion coefficient and air permeability such as pore tortuosity-connectivity factor (X_G) and equivalent pore diameter (d_G) for gas flow. Both undisturbed and repacked samples were used for characterizing soil pore networks. In MFXCT analysis, the pore structural parameters such as effective pore diameter (d_{MFXCT}), pore tortuosity (T_{MFXCT}), and coordination number (C_{MFXCT}) were measured. Results showed the moisture content affected clearly pore structural parameters, T_{MFXCT} and C_{MFXCT} decreased with increasing soil air filled porosity, however, measured d_{MFXCT} were independent on the moisture content. For both undisturbed and disturbed samples, the measured T_{MFXCT} and X_G became close and plotted in a narrow range between 1:1.5 and 1.5:1. On the other hand, high variations were observed between d_{MFXCT} and d_G, indicating that the indirectly estimated equivalent pore diameter from soil gas transport parameters does not correspond to the mean diameter of soil macropore.

Keywords: Pore Structural Parameters, Microfocus X-ray Computed Tomography (MFXCT), Volcanic Ash Soil, Macropore, Soil-Gas Diffusion, Air Permeability

1. INTRODUCTION

Knowledge and understanding of gas transport processes in porous media are important for the environmental risk assessment and design of remediation methods at the contaminated sites. For examples, estimating emission of greenhouse gases from solid waste landfill site [1], estimating contaminates at polluted sites and estimating aeration rates in agricultural soils [2]. Gas transport in soil occurs through the soil pore network, which is mainly controlled by soil pore structural parameters such as pore size distribution, pore tortuosity and pore coordination number. Non-destructive methods, such as an X-ray computed tomography (CT) has become a powerful technique to identify three-dimensional characterization of soil pore [3,4]. Recently, numerous studies have examined pore structural parameters based on the X-ray computed tomography (CT) about porosity [5], pore size distribution [6] and pore network tortuosity [7]. However, there is limited number of studies on visualization and quantification of soil pore network and soil pore networks linked with the indirect pore parameters for gas flow based on measured soil gas diffusion coefficient (D_p) and air permeability (k_a). Naveed [7] measured gas transport parameters (D_p and k_a) for Accusand (Unimin Corp., Ottawa, MN) and Granusil (Unmin Corp., Emmett, ID) and derived the correlations to pore structural parameters from X-ray CT analysis. They suggested that reasonably good agreement in tortuosity values obtained from CT analysis and from gas transport parameters. Similarly, Baniya [8] and Muller [9] found that pore structural parameters derived from X-ray CT were affected by compaction and they fairly predicted gas transport parameters such as soil-gas diffusivities and air permeabilities.

In this study, soil macropore networks with pore diameter ≥ 30 μm were visualized for different moisture contents of volcanic ash soils using MFXCT system. Volcanic ash soils (Andosols) are characterized by unique soil physical properties such as low bulk density, high water retention capacity and high permeability [10]. The gas transport parameters of the soil samples (D_p and k_a) were measured in the laboratory. The objectives of

this study were to (i) evaluate the effects of moisture content on the pore structural parameters and (ii) compare pore structural parameters from MFXCT to the indirectly estimated pore structural parameters such as equivalent pore diameter and tortuosity-connectivity factor for gas flow.

2. MATERAILS AND METHODS

2.1 Materials

Volcanic ash soil (Andosols) collected from the grass-covered field at the University of Tokyo's agricultural site in Nishi-Tokyo City, Japan was used in this study. Both undisturbed and repacked soil sampled from two different depths: 5 cm and 50 cm depth below the surface were examined. The soils physical and chemical properties are shown in Table 1. For repacked soil samples, particle size ($d \leq 2$mm) with field water content (Samples below the 5 cm depth, w = 76 % and samples below the 50 cm depth w = 124 %) were prepared with various dry bulk densities (5 cm depth samples – 0.55 and 0.80 g cm^{-3} and 50 cm depth samples – 0.49 and 0.55 g cm^{-3}) by manual compaction. The samples were directly packed in an acrylic core of height 4.06 cm and diameter 5.61 cm. Undisturbed samples were used in the intact condition. All undisturbed and packed samples (FWC) were saturated and subsequently drained to the desired soil-water potential (ψ, cmH_2O) values using a hanging water column (ψ = 0 to –60 cmH_2O), and a pressure chamber (ψ = 100 to -10,000 cmH_2O) by maintaining required moisture contents. Finally, all the samples were prepared in air dry conditions (AD) (ψ < –10,000 cmH_2O) at the constant room temperature of 20°C and relative humidity (RH) = 60%.

2.2 Micro-focus X-ray CT Measurements and Analysis

Visualization of the soil pore structures was carried out using a microfocus X-ray CT (MFXCT) system (inspeXio SMX-90CT, Shimadzu Corp., Japan). At first, soil samples were scanned by MFXCT system with different scanning resolutions viz. 12, 30 and 50 µm/voxels. The scanned slices were reconstructed as a three-dimensional structure (Exfact VR 2.1, Nihon Visual Science, Inc., Japan) with different region of interest (50×50×50, 100×100×100, 200×200×200 and 300×300×300 voxels) and pore structural parameters such as pore diameter, pore tortuosity and pore coordination number with a three-dimensional medial axis (3DMA) method [4,11] (EXFact analysis for porous particles, Nihon Visual Science, Inc., Japan) were analyzed. The 3DMA package analyzes the CT data using the three steps: image segmentation, image skeletonization (construction of medial axis) and medial axis analysis. The details of the 3DMA package for X-ray CT analysis can be referred in earlier publications [4,6-8,11]. For image segmentation, predetermined soil air-filled porosity at different moisture content were used to segment pore and grain spaces. The details of scanning and analysis conditions for the MFXCT system are summarized in Table 2.

Fig.1 exemplifies the Multi-Planner Reconstruction (MPR), and binarized images at 5 cm depth of the undisturbed and repacked volcanic ash samples with different scanning resolution (SR). For each parameter, mean values and distributions of parameters were obtained by fitting normal or lognormal distributions to the results at three ROIs. For each scanning conditions, the effective pore diameter (d_{MFXCT}) was fitted with log normal distribution curve whereas the pore coordination number (C_{MFXCT}) and the pore tortuosity in z direction (T_{MFXCT}) were fitted by normal distribution curves. Typical examples of the effects of scanning resolution on the distribution of pore structure parameters are shown in Fig.2. The result shows that the d_{MFXCT} is more depended on the SR in the MFXCT scanning compared to the pore tortuosity or the pore coordination number. This verified that lower SR size results in lowering the d_{MFXCT}. Similar findings were obtained in a previous study for various loamy soils [8].

All pore structure parameters for undisturbed and repacked samples varied depending on the ROI in the MFXCT scanning (Fig.3). However, such variations decreased with increasing ROI (typically, ROIs ≥ 100×100×100 voxels). For both undisturbed and repacked samples, ROI = 50×50×50 voxels showed high variation due to the limited number of pores in the analysis. The pore structure parameters are generally similar for ROI larger than 200×200×200 voxels. Sometimes, the larger voxels were not used in the analysis due to very large computational complexity for the pore structure analysis software used in the image analysis (EXFact analysis for porous particles, Nihon Visual Science, Inc., Japan). In this study scanning resolution 12 and 30 µm/voxel and ROI = 200 ×200×200 voxels were used for image analysis.

Calculated mean (µ) and standard deviation (σ) values of pore structure parameters for undisturbed and repacked samples with different SR are summarized in Table 3. For all mean pore structural parameters, there were less variations of undisturbed and repacked samples based on µ and σ.

Table 1 Basic physical and chemical properties of the soils used in this study (≤ 2mm fraction)

Soil type	Particle size fraction %			ρ_s g cm^{-3}	ρ_d g cm^{-3}	Φ cm^{3}cm^{-3}	ε_{FWC} cm^{3}cm^{-3}	SOC %	SON %	C/N %	LOI %	Soil condition
	Sand	Silt	Clay									
VAS (5 cm depth)	47	41	12	2.51	0.80	0.68	0.07	0.45	0.04	12.4	31.9	Undisturbed
					0.78	0.69	0.09					
					0.55	0.78	0.36					Repacked
					0.80	0.68	0.07					
VAS (50 cm depth)	49	40	11	2.73	0.49	0.82	0.21	0.58	0.03	17.1	20.6	Undisturbed
					0.49	0.82	0.21					
					0.49	0.82	0.21					
					0.55	0.80	0.11					Repacked

ρ_s : particle density, ρ_d : dry bulk density, Φ: total porosity, ε_{FWC} : air-filled porosity at field water content, SOC: soil organic carbon; SON: soil organic nitrogen; LOI: loss of ignition; VAS: volcanic ash soil

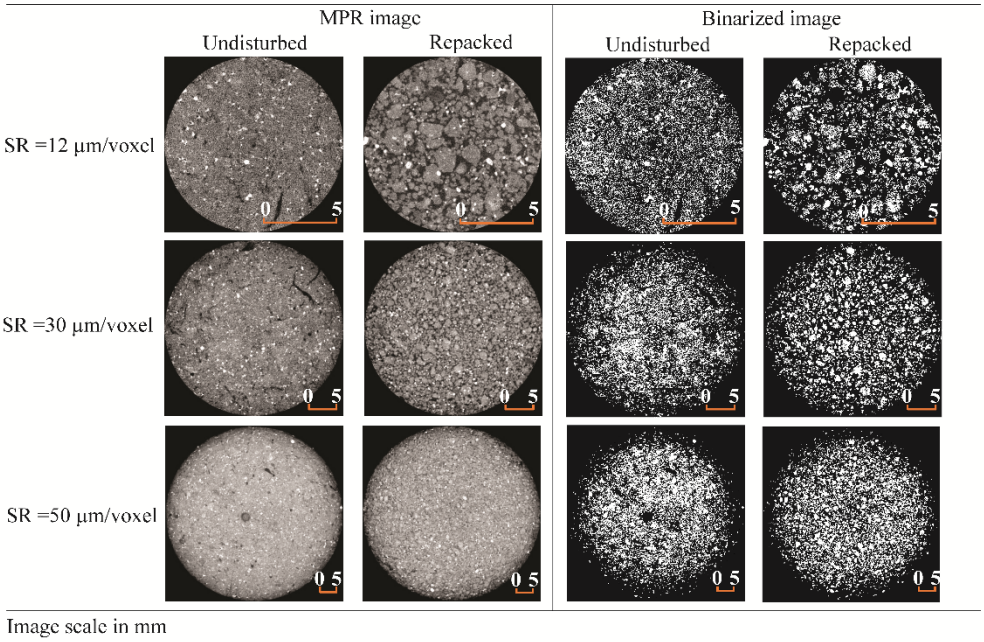

Fig.1 Multiplanar reconstruction image (MPR) and binarized images for undisturbed and repacked volcanic ash samples of dry bulk density 0.80 g cm^{-3} at field water contents.

Table 2 Scanning and analysis conditions for micro focus X-ray computed tomography

Parameter	Setting			Unit
SR	12	30	50	µm/voxel
Average number for scanning	4			
View Number	3600			
FOV (X, Y)	12.0	31.0	50.8	mm
FOV (Z)	6.4	16.4	26.8	mm
Scaling Factor	150			
Image size of slice	1024×1024			voxels
Number of slices	540			
ROI	50×50×50 100×100×100 200×200×200 300×300×300			voxels

SR: scanning resolution, FOV: field of view, ROI: region of interest

2.3 Measurements of Gas Transport Parameters

After the MFXCT scanning, the soil samples were reused to measure the gas transport parameters - the soil-gas diffusion coefficient, D_p (cm^2 s^{-1}) and air permeability, k_a (µm^2) at the constant room temperature of 20°C. The D_p was measured by using the diffusion chamber method developed by [12, 13]. Oxygen gas was used as a tracer gas and the change in the oxygen concentration was measured as a function of time in the diffusion chamber. In this study, the gas diffusion coefficient of oxygen in free air (D_0) at 20°C was taken as 0.20 cm^2 s^{-1} [12, 14] was used to calculate soil gas diffusivity. The k_a was measured by an air permeameter from the Darcy's equation [15] based on the pressure differences across the soil sample and viscosity of the air (1.86×10^{-5} Pa s). The

tortuosity-connectivity from gas transport was calculated using previously developed simple power-law models as given by Eq.(1) [16] whereas equivalent pore diameters were estimated using the relationship between diffusivity (D_p/D_o) and air permeability(k_a) as given by Eq. (2) [17] respectively.

$$X_G = log\left(\frac{D_p}{D_0}\right)/log\varepsilon \quad (1)$$

$$d_G = 2\sqrt{8k_a/(D_p/D_o)} \quad (2)$$

where, X_G and d_G are the pore connectivity-tortuosity factor and equivalent pore diameter for gas flow.

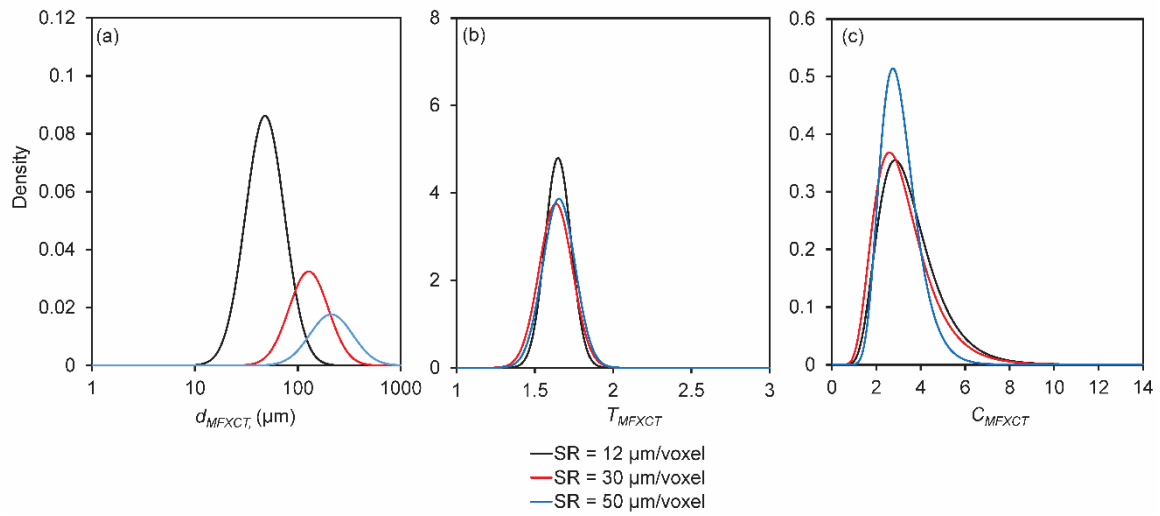

Fig.2 Distribution of pore structure parameters for undisturbed volcanic ash soils of dry bulk density 0.80 g cm^{-3} with different scanning resolution (SR). (a) effective pore diameter (d_{MFXCT}) (b) pore tortuosity (T_{MFXCT}) (c) pore coordination number (C_{MFXCT}). (ROI = 200×200×200 voxels)

Table 3 Summary of pore structure parameters effective pore diameter (d_{MFXCT}), pore tortuosity (T_{MFXCT}) and pore coordination number (C_{MFXCT}) by microfocus X-ray computed Tomography measurements at SR 12 and 30 µm/voxel with region of interest of 200×200×200 voxels

Sample	ρ_d gcm^{-3}	SR 12 µm/voxel						SR 30 µm/voxel					
		d_{MFXCT}		T_{MFXCT}		C_{MFXCT}		d_{MFXCT}		T_{MFXCT}		C_{MFXCT}	
		μ	σ	μ	σ	μ	σ	μ	σ	μ	σ	μ	σ
VAS 5 cm depth (Undisturbed FWC)	0.80	61.0	14.1	-	-	3.49	1.33	176	44.2	-	-	3.25	1.31
VAS 5 cm depth (Undisturbed AD)	0.78	64.0	14.7	-	-	3.17	1.12	170	39.1	-	-	3.18	0.96
VAS 5 cm depth (Repacked FWC)	0.80	59.0	10.5	1.53	0.04	3.39	1.07	160	30.4	1.58	0.06	3.29	1.09
VAS 5 cm depth (Repacked AD)	0.78	59.4	11.1	1.56	0.05	3.44	1.14	165	34.7	1.61	0.06	3.44	1.14
VAS 50 cm depth (Undisturbed FWC)	0.55	57.8	12.1	1.69	0.10	3.10	0.95	242	60.2	1.60	0.06	3.46	1.02
VAS 50 cm depth (Undisturbed AD)	0.80	59.4	12.8	-	-	3.26	1.16	172	42.4	-	-	3.26	1.10
VAS 50 cm depth (Repacked FWC)	0.55	58.2	10.2	1.65	0.08	3.22	0.92	194	31.4	1.73	0.09	3.09	0.80
VAS 50 cm depth (Repacked AD)	0.80	57.6	10.2	1.57	0.05	3.17	0.85	158	29.2	1.58	0.05	3.20	0.86
	0.49	65.8	15.8	1.74	0.23	3.16	0.95	212	59.2	1.76	0.15	3.22	0.91
	0.49	64.8	14.6	1.82	0.14	3.23	1.03	212	60.4	1.85	0.18	3.28	1.01
	0.49	57.6	11.0	1.61	0.07	3.20	0.93	165	26.3	1.68	0.10	3.28	1.0
	0.49	59.0	11.3	1.61	0.07	3.23	1.03	166	36.0	1.67	0.09	3.24	0.91
	0.49	63.8	15.6	1.86	0.17	3.23	1.06	230	63.8	1.79	0.14	3.52	1.18
	0.55	64.8	16.1	2.24	0.39	3.29	1.18	214	58.1	-	-	3.25	1.04
	0.49	55.2	9.3	1.62	0.14	3.17	0.88	218	61.3	1.63	0.07	3.57	1.22
	0.55	56.8	10.2	1.83	0.15	3.16	0.87	176	31.1	1.97	0.15	2.83	0.53

VAS: volcanic ash soils; SR: scanning resolution, ρ_d: dry bulk density, d_{MFXCT}: effective pore diameter, T_{MFXCT}: *pore* tortuosity, C_{MFXCT}: pore coordination number, μ: mean, σ: standard deviation

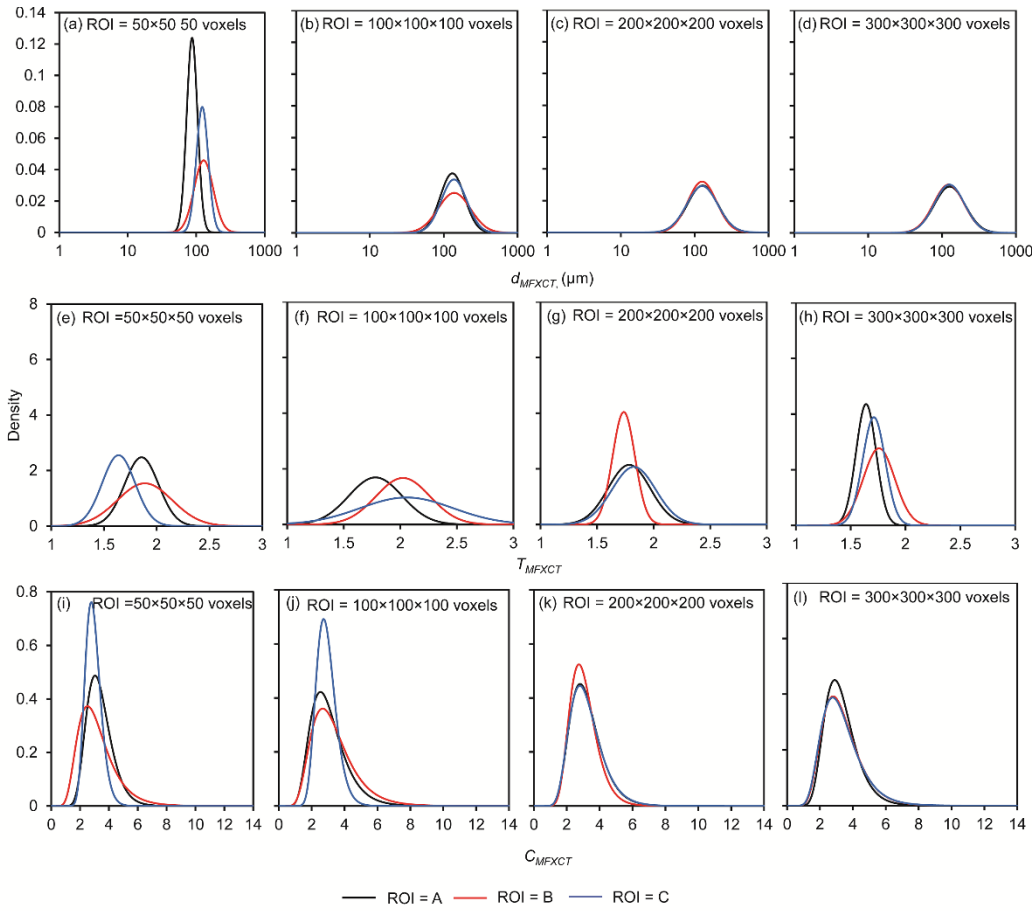

Fig.3 Distribution of pore structure parameters for undisturbed volcanic ash soils of dry bulk density 0.80 g cm^{-3} with different region of interest (ROI) (SR 30 μm/voxel) : (a, e, i) ROI = 50×50×50voxels, (b, f, j) ROI = 100×100×100 voxels, (c, g, k) ROI = 200×200×200 voxels, and (d, h, l) ROI = 300×300×300 voxels and (a), (b), (c) and (d) are effective pore diameter (d_{MFXCT}), (e), (f), (g) and (h) are pore tortuosity (T_{MFXCT}), (i), (j), (k) and (l) are distribution of pore coordination number (C_{MFXCT})

3. RESULTS AND DISCUSSION

3.1 Effects of Moisture Content on Pore Structural Parameters

To clarify the dependence of moisture content, mean values of d_{MFXCT}, T_{MFXCT}, and C_{MFXCT} for all tested samples measured by MFXCT at the scanning conditions of SR = 12 and 30 μm/voxel (ROI = 200×200×200 voxels) were plotted against soil air content (Fig. 4). The mean d_{MFXCT} values from SR = 12 μm/voxel was about 60 μm and those from SR = 30 μm/voxel was about 180 μm.

Mean T_{MFXCT} and C_{MFXCT} values decreased slightly with increasing soil air filled porosities (Figs. 4c-4f) however measure d_{MFXCT} for all tested samples were independent on the moisture content (Fig. 4a and 4b). For comparison, the findings for d_{MFXCT} , T_{MFXCT}, and C_{MFXCT} were obtained in a previous study [8] for variably compacted loam are also included in Figs. 4a-4f. Especially, for those moist samples (low ε), the T_{MFXCT} values become higher than the others. It is supposed that pore space is disconnected due to water. Baniya [8] found that pore structural parameters derived from MFXCT were affected by compaction (d_{MFXCT} and T_{MFXCT} decrease and C_{MFXCT} increase with increasing dry bulk densities). However, in this study T_{MFXCT} and C_{MFXCT} varies slightly with increasing soil air-filled porosities. The difference between the results obtained at different moisture conditions (t-test P > 0.05) for both SR = 12 and 30 μm/voxel were not significant. It was expected that, the pore structure parameters (d_{MFXCT}, T_{MFXCT}, and C_{MFXCT}) would vary with moisture contents so that the derived relation between pore structural parameters from MFXCT with soil air contents also varies. The dependency of pore connectivity tortuosity factor (X_G) and equivalent pore diameter (d_G) on soil air-filled porosities (ε) are shown in Fig. 5a and Fig. 5b respectively. X_G decrease with increasing ε (minimum values on soil air filled contents at PF3)

and increased to a large X_G value at air dry condition. It is interesting that the observed trend was analogue to the previous studies by Resurreccion [18]. However, d_G increase with increasing ε.

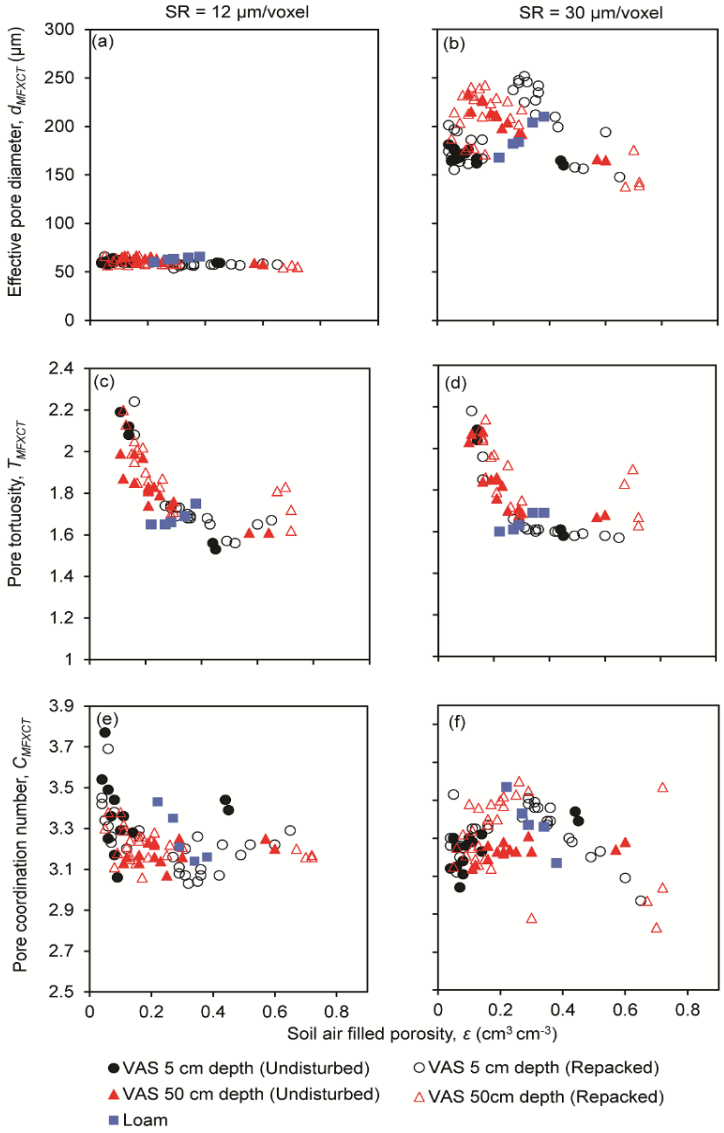

Fig.4 Effects of Moisture contents on pore structural parameters: (a, b) effective pore diameter, $d_{MFXCT,}$ (c, d) pore tortuosity, T_{MFXCT}, and (e, f) pore coordination number, C_{MFXCT}. (a), (c), and (e) were measured at a scanning resolution (SR) of 12 μm/voxel and region of interest (ROI) of 200×200×200 voxels and (b), (d), and (f) were measured at SR = 30 μm/voxel and ROI = 200×200×200 voxels

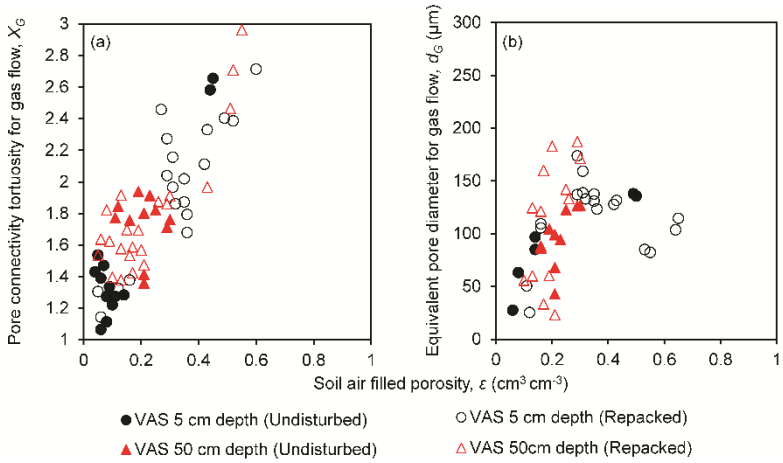

Fig.5 Dependency of (a) pore connectivity tortuosity factor (X_G) and (b) equivalent pore diameter (d_G) for gas flow on soil air-filled porosities (ε)

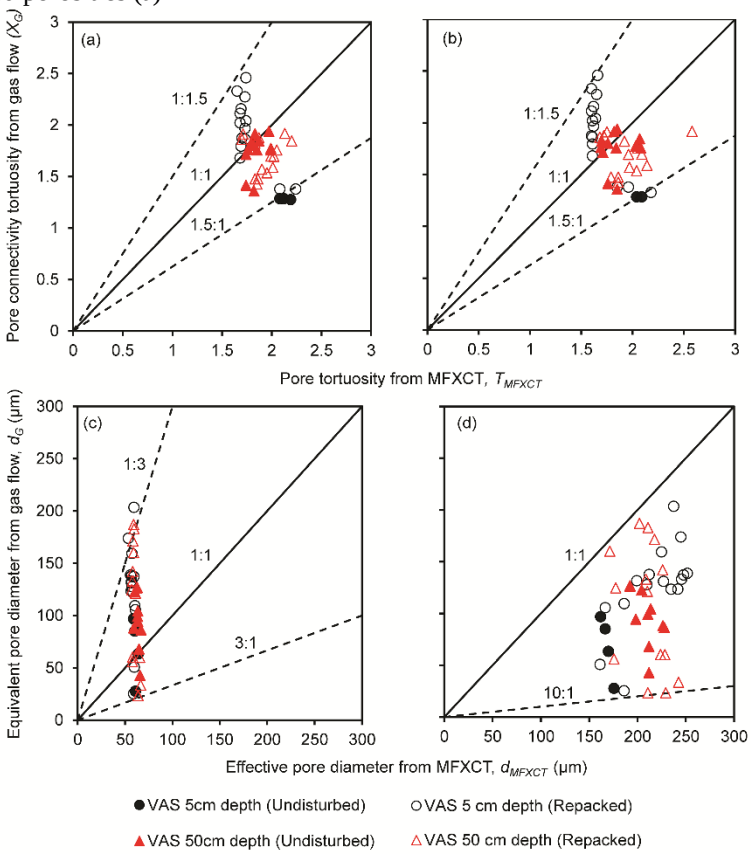

Fig.6 Comparison of pore connectivity tortuosity factor determined from MFXCT (T_{MFXCT}) and from gas transport parameters (X_G) (a) SR = 12 μm/voxel (b) SR = 30 μm/voxel. Comparison of pore diameter from MFXCT (d_{MFXCT}) and from gas transport parameters (d_G) (c) SR = 12 μm/voxel (d) SR = 30 μm/voxel. (Solid line represents 1:1 and dotted lines represents boundary lines).

3.2 Comparison of Pore Structural Parameters from MFXCT and Gas Transport Parameters

For both undisturbed and disturbed volcanic ash samples, the measured pore tortuosity from MFXCT (T_{MFXCT}) and estimated pore connectivity tortuosity factor (X_G) became close and plotted in a narrow range between 1:1.5 and 1.5:1 (Figs. 6a and 6b). This correlation gives the indirectly estimated tortuosity-connectivity factor well represents the tortuosity of soil macropore network. Naveed [7] had also reported that reasonably good agreement between the pore characteristic parameter tortuosity determined from MFXCT analysis and gas transport parameters. On the other hand, there was no correlations observed between effective pore diameters from MFXCT (d_{MFXCT}) and equivalent pore diameters for gas flow (d_G) (Figs. 6c and 6d).

This indicate that indirectly estimated pore diameters do not correspond to the diameter of macropore network in volcanic ash soil. It has been reported that volcanic ash soils have a typical dual pore structure consisting of interpore (corresponding to macropores in this study) and intra pores (micropores in aggregates) [19]. The d_G would not be evaluated by macropore network (i.e., d_{MFXCT}) but be controlled significantly by interpore network of volcanic ash soils.

4. CONCLUSION

The effects of moisture content on pore structural parameters for undisturbed and disturbed volcanic ash soils based on the microfocus X-ray CT were analysed and compared the MFXCT derived parameters to indirectly estimated parameters from soil-gas diffusion coefficient and air permeability. Mean pore tortuosity and pore coordination number decreased with increasing soil air filled porosity, however pore diameter was independent on moisture content. Indirectly estimated pore diameter does not correspond to the mean pore diameter of soil macropore, on the other hand, pore connectivity tortuosity factor well represents the tortuosity of soil macropore from MFXCT. Further studies are needed to characterize soil pore network and its correlation to gas transport parameters in soil.

5. ACKNOWLEDGMENTS

This study was partially supported by a JST-JICA Science and Technology Research Partnership for Sustainable Development (SATREPS) project and was made possible by the 'Providing New Insight into Interactions Between Soil Functions and Structure' (PROTINUS)-project in the framework of H2020.

6. REFERENCES

[1] Kruse C. W., Moldrup P., and Iversen N., Modeling Diffusion and Reaction in Soils .2. Atmospheric Methane Diffusion and Consumption in a Forest Soil, Soil Sci., Vol. 161, No. 6, 1996, pp.355-365.

[2] Poulsen T. G., Blendstrup H., and Schjønning P., Air Permeability in Repacked Porous Media with Variable Structure-Forming Potential, Vadose Zo. J., Vol. 7, No. 4, 2008, pp.1139-1143.

[3] Otani J., Mukunoki T., and Obara Y., Application of X-Ray CT Method for Characterization of Failure in Soils., Soils Found., Vol. 40, No. 2, 2000, pp.111-118.

[4] Hamamoto S., Moldrup P., Kawamoto K., Sakaki T., Nishimura T., and Komatsu T., Pore Network Structure Linked by X-Ray CT to Particle Characteristics and Transport Parameters, Soils Found., Vol. 56, No. 4, 2016, pp.676-690.

[5] Anderson S. H., Peyton R. L., and Gantzer C. J., Evaluation of Constructed and Natural Soil Macropores Using X-Ray Computed Tomography, Geoderma, Vol. 46, No. 1-3, 1990, pp.13-29.

[6] Lindquist W. B.,Venkatarangan A., Dunsmuir J.,and Wong T., Pore and Throat Size Distributions Measured from Synchrotron X-Ray Tomographic Images of Fontainebleau Sandstones, J. Geophys. Res. Solid Earth, Vol. 105, No. B9, 2000, pp.21509-21527.

[7] Naveed M., Hamamoto S., Kawamoto K., Sakaki T., Takahashi M., Komatsu T., Moldrup P., Lamandé M., Wildenschild D., Prodanović M., and De Jonge L.W., Correlating Gas Transport Parameters and X-Ray Computed Tomography Measurements in Porous Media, Soil Sci., Vol. 178, No. 2, 2013, pp.60-68.

[8] Baniya A., Kawamoto K., Hamamoto S., Sakaki T., Saito T., Müller K., Moldrup P., and Komatsu T., Linking Pore Network Structure Derived by Microfocus X-Ray CT to Mass Transport Parameters in Differently Compacted Loamy Soils, Soil Res., Vol. 57, No. 6, 2019, pp.642-656.

[9] Müller K., Dal Ferro N., Katuwal S., Tregurtha C., Zanini F., Carmignato S., Wollesen De Jonge L., Moldrup P., and Morari F., Effect of Long-Term Irrigation and Tillage Practices on X-Ray CT and Gas Transport Derived Pore-Network Characteristics, Soil Res., Volume 57, No 6, 2018, pp.657-669.

[10] Duwig C., Prado B., Tinet A.-J., Delmas P., Dal Ferro N., Vandervaere J.P., Denis H., Charrier P., Gastelum Strozzi A., and Morari F. C., Impacts of Land Use on Hydrodynamic Properties and Pore Architecture of Volcanic Soils from the Mexican Highlands, Soil Res., Vol. 57, No. 6, 2019, pp.629-641.

[11] Lindquist W. B. and Venkatarangan A., Investigating 3D Geometry of Porous Media from High Resolution Images, Phys. Chem. Earth, Part A Solid Earth Geod., Vol. 24, No. 7, 1999, pp.593-599.

[12] Currie J. A., Gaseous Diffusion in Porous Media Part 1. - A Non-Steady State Method, Br. J. Appl. Phys., Vol. 11, No. 8, 1960, pp.314-317.

[13] Osozawa S., Measurement of Soil-Gas Diffusion Coefficient for Soil Diagnosis, SPCPG, Vol. 55, 1987, pp.53-60.

[14] Gliński J. and Stępniewski W., Soil aeration

and its role for plants, 1985. CRC Press, Inc., 1985, pp.52-94.

[15] Iverson B. V,Schjonning P.,Poulsen T. G.,and Moldrup P., In Situ, on-Site and Laboratory Measurements of Soil Air Permeability: Boundary Conditions and Measurement Scale, Soil Sci., Vol. 166, No. 2, 2001, pp.97-106.

[16] Buckingham E., Contributions to Our Knowledge of the Aeration of Soils, 1904. U.S. Dept. of Agriculture, Bureau of Soils, 1904, pp.33-40.

[17] Millington R. J. and Quirk J. P., Formation Factor and Permeability Equations, Nature, Vol. 202, No. 4928, 1964, pp.143-145.

[18] Resurreccion A. C.,Moldrup P., Kawamoto K.,Yoshikawa S., Rolston D. E., and Komatsu T., Variable Pore Connectivity Factor Model for Gas Diffusivity in Unsaturated, Aggregated Soil, Vadose Zo. J., Vol. 7, No. 2, 2008, pp.397-405.

[19] Kawamoto K., Moldrup P., Komatsu T., de Jonge L.W., and Oda M., Water repellency of aggregate size fractions of a volcanic ash soil. Soil Sci. Soc. Am. J., Vol. 71, 2007, pp.1658-1666.